
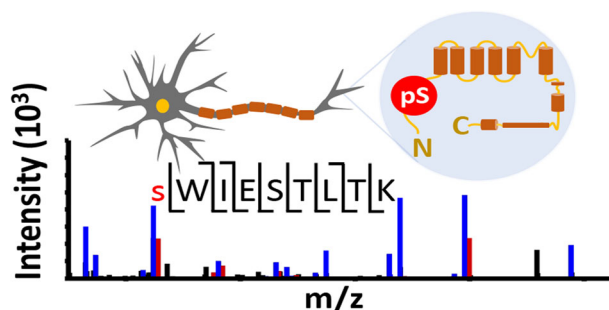


# Investigating Phosphorylation Patterns of the Ion Channel TRPM7 Using Multiple Extraction and Enrichment Techniques Reveals New Phosphosites

Thu T. A. Nguyen,<sup>1</sup> Wenping Li,<sup>2</sup> Thomas J. Park,<sup>2</sup> Liang-Wei Gong,<sup>2</sup>  
Stephanie M. Cologna<sup>1,2</sup> 

<sup>1</sup>Department of Chemistry, University of Illinois at Chicago, Chicago, IL 60607, USA

<sup>2</sup>Laboratory for Integrative Neuroscience, University of Illinois at Chicago, Chicago, IL 60607, USA



**Abstract.** The study of membrane proteins, and in particular ion channels, is crucial to understanding cellular function. Mass spectrometry-based approaches including bottom-up strategies to study membrane proteins have been successful yet still can remain challenging. In this study, we sought to evaluate the phosphorylation patterns of the ion channel TRPM7 which is involved in a range of critical physiological functions. To overcome extraction obstacles associ-

ated with analyzing membrane proteins, we incorporated the use of 5% SDS solubilization coupled with SCAD and S-Trap digestion methods to eliminate detergent interference in downstream LC-MS/MS analysis. We found that the SCAD method was more efficient, yielding 84% of the overall identified proteins; however, the variability was greater than the S-Trap method. Using both methods together with TiO<sub>2</sub> and Fe-NTA phospho-enrichment protocols, we successfully observed the phosphorylation pattern of TRPM7 in a transfected cell line. An average of 22 ± 6% of the TRPM7 amino acid sequence was observed. In addition to several previously reported phosphorylation sites, we identified six new phosphosites (S5, S233, S554, S824, T1265, and S1401), providing new targets for further functional analyses of TRPM7.

**Keywords:** TRPM7, SCAD, S-Trap, Phosphorylation, Post-translational modifications, Peptide enrichment, Phosphoproteomics, Membrane proteins

Received: 4 February 2019/Revised: 9 April 2019/Accepted: 10 April 2019/Published Online: 28 May 2019

## Introduction

Although accounting for only 20–30% of open reading frames [1], membrane proteins are responsible for many important cellular functions including cellular defense, communication, and ion regulation. More than 50% of drug targets are membrane proteins, with the majority being G protein-coupled receptors (GPCRs), nuclear receptors, and ion

channels [2]. Of all membrane proteins, ion channels are uniquely important to excitable cells, including neurons and muscle cells. Crucial roles of ion channels include (i) building up membrane potential, (ii) transmitting electrical signals, (iii) regulating cell volume through maintaining electrolytic balance, and (iv) triggering intracellular signaling pathways [3]. Additionally, many neurological and neuromuscular disorders have also been linked to ion channel dysfunction [3], yet many have dual roles in activating neuroprotection and neurodegeneration [4].

Transient receptor potential cation channel subfamily M member 7 (TRPM7) is a nonselective cation channel that is known for its role in Ca<sup>2+</sup> and Mg<sup>2+</sup> influx in synaptic vesicle recycling [5]. Through structural and sequence analysis, it has

**Electronic supplementary material** The online version of this article (<https://doi.org/10.1007/s13361-019-02223-5>) contains supplementary material, which is available to authorized users.

Correspondence to: Stephanie Cologna; e-mail: [cologna@uic.edu](mailto:cologna@uic.edu)

been determined that TRPM7 also resembles a conventional protein kinase with diverse substrates such as myosin heavy chain IIA, annexin, and phospholipase C gamma-2, and can be regulated by phosphatidylinositol(4,5)biphosphate (PIP<sub>2</sub>), demonstrating the significance of this protein in a large range of physiological functions [5–8]. TRPM7 has also been known to play major roles in pathological conditions such as cancer, ischemic stroke, hypertension, and neurodegeneration [9]. Specifically, mutation of tyrosine 1482 to a neutral amino acid, preventing phosphorylation, has been thought to alter the activity of TRPM7 in some amyotrophic lateral sclerosis and Parkinsonism-dementia patients [10].

Despite the importance of ion channels and other membrane proteins in cellular homeostasis, their mechanisms and functions are still poorly understood. Since these proteins are hydrophobic in nature, biochemical and biophysical studies, including mass spectrometry (MS), have faced major challenges in downstream analysis and characterization. To overcome these challenges, several efforts have been made to develop new protocols including detergents and detergent-lipid micelles to maximize the solubilization of membrane proteins, and limit the interference with detection methods [11–14]. Major advancements have also been made to evaluate native states and structures of membrane proteins via MS by utilizing nanodiscs and other solubilizing or stabilizing agents [15]. In bottom-up proteomics, most studies rely on detergents, commonly sodium dodecyl sulfate (SDS), for solubilization and multiple stages of sample clean-up methods to eliminate micelles and polymeric interferences [16, 17]. In studies of a single protein target, often these studies involve immunoprecipitation to further enhance the signal and abundance of the protein of interest. However, high concentration of detergents and the presence of micelles can compromise the binding capabilities of antibodies and protein-antibody interactions [18, 19]. Furthermore, many membrane proteins lack specific antibodies which makes downstream detection difficult.

Recently, a new method termed surfactant and chaotropic agent assisted sequential extraction/on-pellet digestion (SCAD) was introduced, showing an improvement in protein extraction, coverage, and peptide recovery in comparison with commonly used filter-aided sample pre and urea extractions [20]. Relatedly, the commercially available suspension-trap (S-Trap) technology has recently been reported to provide excellent proteome coverage in bottom-up proteomic studies [16, 21, 22]. In the current study, we sought to optimize a method for solubilization, recovery, and MS-based measurement of TRPM7. Therefore, we evaluated both SCAD and S-Trap approaches to identify TRPM7 in a transfected cell line. Additionally, we were interested in studying the phosphorylation pattern of TRPM7 and included enrichment strategies to identify novel phosphorylation sights that may provide insight into physiological and pathological characteristics of TRPM7.

## Methods

All solvents and chemicals were purchased from Sigma-Aldrich (St. Louis, MO), unless otherwise specified.

### *Cell Culture, Transfection, and Lysis*

HEK293 cells were cultured in DMEM (Thermo Scientific, Waltham, MA) and supplemented with 10% FBS, 0.1 mM MEM non-essential amino acids, 6 mM L-glutamine, 1 mM MEM sodium pyruvate, 1% pen-strep, and 500 µg/ml Geneticin (Thermo Fisher Scientific). Cells, which typically reached 80% confluence every 3 days, were treated with trypsin-EDTA and passaged to a 1:10 ratio for general maintenance. All cell cultures were incubated at 37 °C in 5% CO<sub>2</sub>/95% O<sub>2</sub>.

HEK 293 cells do not natively express high levels of TRPM7. To overexpress TRPM7 in HEK 293 cells, a plasmid containing N-flag-TPRM7 mouse sequence was transfected using the polyethylenimine (PEI)-mediated transfection method [23]. Cells were seeded onto 15-cm petri dishes and transfection occurred over a 24-h period. Fresh complete media supplemented with 4-mM sodium butyrate, which enhances protein expression [24, 25], was replaced with fresh media 6 h post-transfection. Cells overexpressing TPRM7 were harvested 48 h post-transfection, washed with PBS, and flash frozen in liquid nitrogen.

To generate protein lysates, 200 µL of 5% SDS in 50 mM of triethylammonium bicarbonate (TEAB) with a protease inhibitor cocktail (Roche, Basel, Switzerland) and phosphatase inhibitors (1-mM NaF, 1-mM PMSF, 1-mM sodium orthovanadate, 10-mM sodium pyrophosphate, and β-glycerophosphate) were added to each frozen cell pellet, which contained approximately 10 million cells. Lysates were sonicated on ice three times for 10 pulses each, followed by 2-min rest between repeat cycles. Power was at 40% using a Q125 sonicator (Qsonica, Newtown, CT). After 10 min of centrifugation at 14,000×g, the supernatant was transferred to a new tube. Lysate concentration was determined by using the bicinchoninic acid (BCA) protein assay (Thermo Scientific, Waltham, MA) according to the manufacturer's protocol. Three replicates of each experiment were performed.

### *S-Trap Preparation*

Sample preparation was carried out using a S-Trap mini spin column digestion protocol (Protifi, Huntington, NY). Four aliquots, each containing 300 µg of protein, were diluted to 50 µL with lysis buffer (5% SDS in 50-mM TEAB) corresponding to a total of 1.2 mg of protein processed for each replicate. Dithiothreitol (DTT) was added to each aliquot to a final concentration of 20 mM and heated at 95 °C for 10 min. After cooling to room temperature, samples were alkylated in the dark for 40 min with 40 mM of iodoacetamide (IoAc). Then, 5 µL of 12% phosphoric acid and 350 µL of binding buffer (90% methanol, 100-mM TEAB) were added to each sample and mixed appropriately. Samples were loaded onto

spin columns and centrifuged at 4000×g for 30 s. After four washes, 125 μL of 50-mM TEAB and 6 μg of trypsin (1:50 ratio) were added to the trap and incubated overnight. Peptides were then eluted with 80 μL of each of the following: 50-mM TEAB, 0.2% formic acid (FA), and 50% ACN in 0.2% FA with centrifugation at 1000×g after each elution step. All elution fractions were pooled and dried under vacuum.

### SCAD Preparation

SCAD was carried out based on a previous protocol described by Ma et. al [20] with slight modifications. To minimize the variation between the preparation methods, lysates used for S-Trap, which had higher concentration of SDS than the published method, were used for SCAD. Similar to S-Trap, SCAD was performed in four aliquots with a total of 1.2-mg protein lysate being processed. Samples were first reduced and alkylated, respectively, by an incubation at 55 °C for 30 min with 10-mM DTT, followed by an incubation with 50-mM IAc in the dark, at room temperature. SDS removal was done via protein precipitation with acetone. Cold acetone was added to the samples to achieve a final concentration of 80% (v/v). Samples were left to precipitate overnight at – 20 °C and centrifuged at 16,000×g for 15 min to remove the supernatant. Each sample was then incubated at – 20 °C with 80% acetone/water (v/v) mixture for 2 h, and the centrifugation step was repeated. Pellets were left to dry at room temperature for 30 min. Next, 50 μL of 6M urea, containing 3 μg of LysC (1:100 enzyme:protein ratio) was added to the resulting pellets for 2 h for digestion at 28 °C. Samples were diluted with 450 μL of 100-mM ammonium bicarbonate (ABC) to reach a final concentration of 1M urea. Trypsin (6 μg) was added and samples were incubated at 37 °C overnight.

For SCAD-prepared samples, a desalting step was carried out using OASIS HLB 1 cc Vac Cartridge (30-mg sorbent, 30 μm particle size) (Waters Corporation, Milford, MA). Prior to desalting, samples were dried and re-suspended in 0.1% FA. The column was first washed with 80% ACN in 0.1% FA, followed by equilibration with 0.1% FA. Samples were loaded/reloaded three times to minimize sample loss, washed five times with 0.1% FA, eluted with 70% ACN in 0.1% FA, and dried before phosphopeptide enrichment.

### Phosphopeptide Enrichment

Phosphopeptide enrichment of tryptically digested peptides was done using High-Select Titanium dioxide (TiO<sub>2</sub>) and High-Select Ferric Nitrotriacetate (Fe-NTA) Phosphopeptide Enrichment Kits (Thermo Scientific, Waltham, MA) according to the manufacturer's recommendations.

**Titanium Dioxide** A total of 600 μg of protein lysate from each sample preparation was re-suspended in 150 μL of binding/equilibration buffer (pH < 3) and loaded onto a pre-equilibrated spin tip. Using centrifugal force at 1000×g for 5 min, samples eluted through the beads. The flow-through

was saved and reloaded once, then saved for MS analysis. Tips were washed five times, alternating between binding/equilibration buffer and wash buffer, with a final wash by LC-MS-grade water. Each wash was done by adding 20 μL of buffer and centrifuged at 3000×g for 2 min. Lastly, phosphopeptides were eluted twice using 50 μL of elution buffer with high pH. Samples were immediately dried in a vacuum concentrator.

**Ferric Nitrotriacetate** The Fe-NTA spin column was equilibrated with binding/wash buffer; the bottom was capped with a Luer plug. A total of 600 μg of protein was re-suspended in 200 μL of binding/wash buffer (pH < 3), loaded on to the column, and incubated with mild mixing, by tapping the bottom every 10 min, for a total of 30 min. Next, the column was centrifuged at 1000×g for 30 s. The flow-through was saved for MS analysis. The resin was washed three times with 200 μL of binding/wash buffer and once with LC-MS grade water. Each washing step included centrifugation at 1000×g for 30 s. Phosphopeptides were eluted twice with 100 μL of elution buffer using 30 s of centrifugation at 1000×g. Samples were immediately dried using a vacuum concentrator.

### Synthetic Peptides

Four standard peptides were purchased from GenScript (Nanjing, China). The sequences of the synthetic peptides were sWIESTLTK, NTSsSTPQLR, LGSSPNSSPHMSsPPTK, and SHLEsTTKDQEPIFYK. Each aliquot of 1 mg of peptide was re-suspended in 1 mL of 0.1% FA. Next, an equivalent of 5 nmol was aliquoted, diluted to 50 μL, desalted with Ziptip C<sub>18</sub> (Millipore, Burlington, MA), and vacuum dried. Samples were re-suspended in 100 μL of 0.1% FA to a final concentration of 5000 fmol/μL. Subsequently, peptide solutions were diluted to 500 fmol/μL with 0.1% FA. The final dilution was done using 10% ACN in 0.2% FA, for a final concentration of 250 fmol/μL of peptides in 5% ACN 0.1% FA. A total of 125 fmol of each standard phosphopeptide was analyzed by LC-MS/MS.

### LC-MS Acquisition

All samples were desalted and concentrated with OMIX C<sub>18</sub> tips (Agilent Technologies, Santa Clara, CA), dried, and re-suspended in 0.1% FA prior to analysis using a Q Exactive mass spectrometer (Thermo Fisher Scientific, Bremen, Germany) coupled with an Agilent 1260 Infinity nanoLC system (Agilent Technologies, Santa Clara, CA). Each sample was re-suspended in 0.1% formic acid for analysis, 60 μL for enriched phosphopeptides and 160 μL for the combined flowthrough (FT) samples. Respectively, 2.5 μL of phospho-sample, and 0.5 μL of FT (~250ng) was loaded onto a PEEK trapping cartridge (5 × 0.3 mm, Zorbax 300 SB C8, C18, and SCX; Agilent Technologies, Santa Clara, CA) and washed with solvent A (0.1% FA) for 10 min at 2 μL/min flowrate. Next,

samples were loaded onto an Agilent Zorbax 300SB-C18 column ( $0.075 \times 150$  mm,  $3.5 \mu\text{m}$   $300 \text{ \AA}$ ) at 5% B (0.1% FA in ACN). Separation was carried out using a 120-min gradient with a flowrate of  $0.25 \mu\text{L}/\text{min}$ . Gradient conditions were 90 min from 5 to 25% B, 30 min from 25 to 60% B, and a 0.1-min increase from 60 to 90% B. The system was then maintained at 90% B for 10 min prior to a 15-min re-equilibration segment at 5% B prior to the next run. Mass spectra were collected using data-dependent acquisition (DDA) with a capillary temperature of  $250 \text{ }^\circ\text{C}$  and spray voltage of 1.5 kV. Full MS scans were collected at a mass resolution of 70,000 with a scan range of 375–1600  $m/z$ . Automatic gain control (AGC) target was set at  $1 \times 10^6$  for a maximum injection time (IT) of 100 ms. The top ten most intense peaks were selected for MS/MS analysis, with an isolation width of 1.5  $m/z$ . MS/MS spectra were acquired at a resolution of 17,500, ACG target  $1 \times 10^5$ , maximum IT of 50 ms. The first fixed mass was set at 100  $m/z$ . Parent ions were fragmented at a normalized collision energy (NCE) of 27%. Dynamic exclusion was set for 20 s. Parent ions with charges of 1 and larger than 6 were excluded.

### Data Analysis

Raw files were searched with Proteome Discoverer 2.2 (Thermo Fisher Scientific, Waltham, MA) using the Sequest HT search engine against the UniProt *Mus musculus* database (22,286 gene sequence; downloaded April 27, 2017). Mass error tolerance was set to 10 ppm for precursors, cleaved by trypsin, allowing a maximum of two missed cleavages, with sequence lengths between 6 and 144 amino acids. Fragment masses were searched with a tolerance of  $\pm 0.02$  Da. Dynamic modifications included oxidation (M), phosphorylation (S, T, Y), and acetylation (N-terminus). Carbamidomethylation was set as a static modification (C). Both peptides and PSMs were set to a target false discovery rate (FDR) of  $\leq 0.05$  for peptide-spectrum matches with moderate confidence and  $\leq 0.01$  for matches with high confidence. PtmRS was also evaluated for best phospho-site probability. Newly reported phosphorylation sites were manually interpreted.

Venn diagrams of protein IDs and matched peptides versus phosphorylation were made using Proteome Discoverer. Statistical analysis was carried out in GraphPad Prism (San Diego, CA). Identified phosphosites from this dataset were compared with the PhosphoSitePlus tool (Cell Signaling Technology Inc., Danvers, MA, <http://www.phosphosite.org>) and recent publications [26, 27] to determine novel phosphosites. All data is deposited in the MassIVE repository (<ftp://massive.ucsd.edu/MSV000083384>).

## Results and Discussion

In this study, we aimed to optimize a methodology to analyze the critical ion channel, TRPM7, by mass spectrometry including mapping phosphorylation sites as a means to gain insight to potential protein function. To this end, we evaluated two

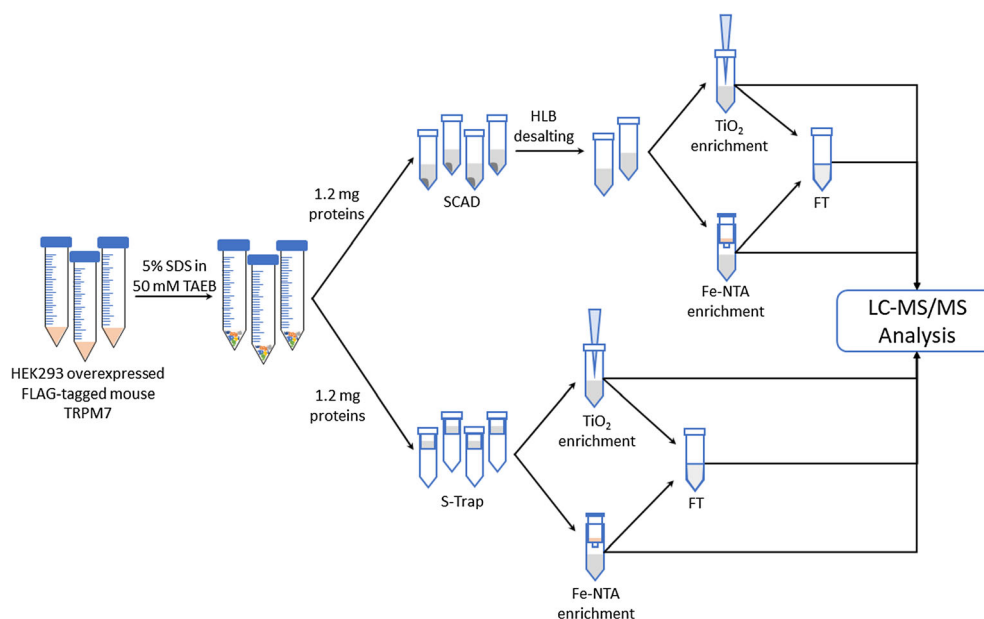
different sample preparation and digestions methods namely, S-Trap and SCAD. Furthermore, we incorporated two phospho-enrichment methods,  $\text{TiO}_2$  and Fe-NTA, to enrich for phosphorylated peptides. The most optimal method would allow for the detection a large portion of the protein and result in maximum phosphorylation site identification with the potential of identifying new sites. The workflow used for this study can be found in Fig. 1. HEK293 cells were transfected with TRPM7 followed by lysis, digestion, enrichment, and detection.

### Comparison of SCAD Versus S-Trap in Extraction Efficiency

To evaluate the overall protein yield for each digestion method, the total number of protein IDs was compared for all three replicates (Fig. 2a). The total number of unique protein identifications from both methods was 10,837, of which 84% (9117 proteins) were identified using SCAD, whereas 66% (7149 proteins) of the total proteins were found using the S-Trap preparation method. Additionally, we evaluated the number of peptides identified in each sample preparation method (Fig. 2b). The number of sequenced peptides from each method was compared, showing 59% of peptides (25,252 out of 43,007 peptides) were observed in SCAD samples. Conversely, data collected following S-Trap preparation resulted in the identification of 41% of the observed peptides (17,755 peptides).

It is important to note that one limitation to this comparison is the difference in enzymes used for the SCAD and S-Trap. Specifically, for SCAD, both LysC and trypsin were used whereas S-Trap only incorporated trypsin digestion. In a preliminary experiment using the SCAD method with only trypsin as the proteolytic enzyme, the number of phosphorylated residues and the protein sequence coverage was not changed for TRPM7. There was, however, an increase in the number of missed cleavages, notably one missed cleavage, as would be expected. As a result, multiple candidate phosphosites were present on the same peptide thereby lowering the probability of phosphorylation for each residue. Regarding whole proteome coverage in our preliminary testing, SCAD results when using trypsin only, indicate the majority of peptides identified were those with one missed cleavage, whereas in S-Trap experiments using only trypsin, the majority of peptides assigned has zero missed cleavages. The total number of proteins identified using only trypsin in both methods was similar ( $\sim 88\%$  overlap). We conclude from these results that for the SCAD method, the improvement observed with combined proteolysis lies mostly in peptide length and not in overall proteome coverage.

The two digestion methods had a high overlap in the proteins identified (ca. 50%). Of the total number of overlapping peptides, 14% of the total peptide assignments were shared between the two methods. Of the common peptides identified in both sample preparation methods, 28% were phosphorylated (1717 peptides). Since the majority of phosphopeptides were

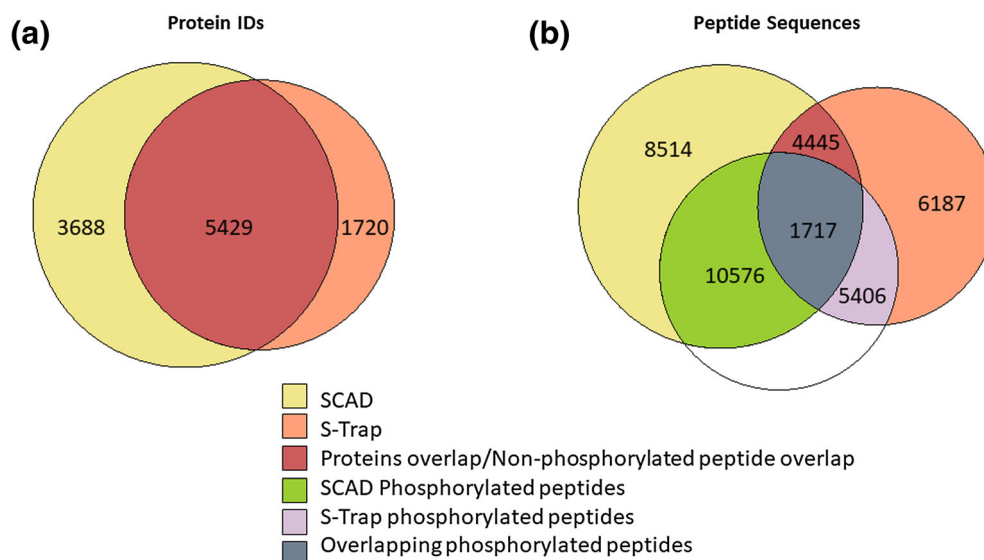


**Figure 1.** Experimental workflow. A total of 1.2 mg of starting material was tryptically digested with either S-Trap or SCAD. Sample processed with SCAD went through an extra step of desalting using HLB cartridges. Next, samples were divided in halves for TiO<sub>2</sub> and Fe-NTA phospho-enrichment. FTs from both enrichments were saved for analysis. The entire workflow was repeated three times with three different cell pellets for biological replicates

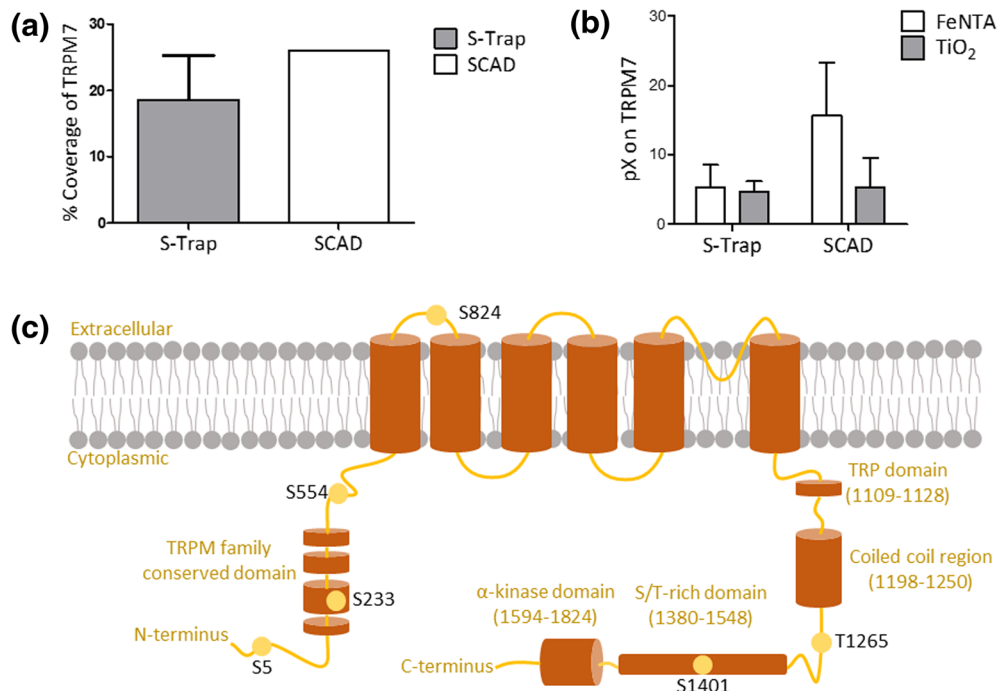
found to be unique to each method (60% in SCAD and 31% in S-Trap), the use of both digestion methods, in combination, was considered to be crucial for the identification of phospho-residues for whole proteome analysis (Fig. 2b).

Furthermore, the effectiveness of these two methods in terms of membrane protein isolation and recovery was analyzed by graphing the identified proteins based on their respective cellular components (Figs. S1 and S2). We observe that the

number of proteins identified and mapped primarily related to the membrane, cytoplasm, and nucleus (Fig. S1). Membrane proteins accounted for approximately 19% of the total proteins identified (Fig. S2). This is consistent with the amount of membrane genes estimated from earlier study [1]. Thus, we conclude that both the SCAD and S-Trap methods provide efficient tools for recovering membrane proteins for MS analysis.



**Figure 2.** Digestion method comparison. SCAD and S-Trap were compared on the overall protein IDs, peptide sequences, and identified phosphorylated peptides. (a) Total number of proteins found in all three repeats were shown for SCAD (yellow), S-Trap (bright orange), with an overlapping of 54,297 proteins (red). (b) Overlapping of peptide sequences found in each digestion method as well as found phosphorylated peptides. It was found that 1717 phosphorylated sequence were matched in both methods of digestion (gray). 10,576 unique phosphorylated sequences were found in SCAD (green), and 5406 (pink) were found in S-Trap. Non-phosphorylated peptides (4445 sequences) identified in both methods were presented in red



**Figure 3.** Detection of TRPM7. The efficiency of digestion methods (SCAD versus S-Trap) and phospho-enrichment methods (TiO<sub>2</sub> versus Fe-NTA) was compared in terms of TRPM7 detection. **(a)** A bar graph of percent TRPM7 coverage using different methods. **(b)** Number of phosphorylated residues confirmed by MS/MS for each pair of methods. Each column represented a mean with standard deviation from all three replicates. Mean percent coverage and phosphorylation sites of TRPM7 by TiO<sub>2</sub> enrichment (gray) for each digestion method were graphed against what was found using Fe-NTA enrichment (white) method. **(c)** Map of new phosphosites identified on TRPM7 proteins (yellow circles)

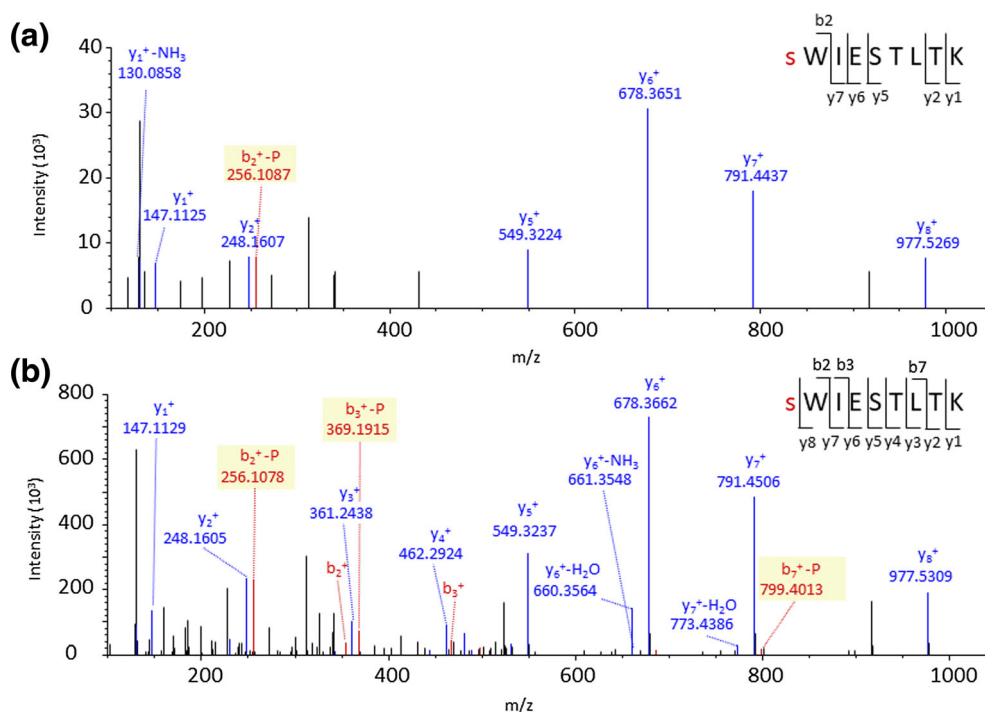
### Detection of TRPM7 Using SCAD and S-Trap

Given that the overall goal of this study was to be able to analyze TRPM7 and potential phosphosites, we next evaluated this aspect (Fig. 3). The success in TRPM7 extraction by each method was first analyzed via the percent amino acid sequence coverage of the protein (Fig. 3a). All three fractions (TiO<sub>2</sub>, Fe-NTA, and FT) were searched together for sequence coverage analysis. Comparing the means and standard deviations (SD) of the percentage of TRPM7 coverage from each of the three runs, suggested that SCAD was a more consistent method and was more efficient in isolating the targeted protein (Fig. 3a). Note that error bars are not discernable from the SCAD analysis owing to the same percent amino acid sequence coverage results in all replicate analyses. The number of phosphorylation sites of the TRPM7 protein was then analyzed by comparing the number of phosphorylated amino acids found from each of the four pairs of methods (Fig. 3b). Each phospho-enrichment method was searched with the corresponding FT fraction for protein and phosphorylation identification, then graphed using the mean and SD. These results indicate that the highest amino acid sequence coverage for TRPM7 is obtained via SCAD. However, there was large variance in the number of phosphosites identified with the different enrichment approaches. Regardless of considering TRPM7 or phosphorylation mapping individually, comparing sequence coverage and phosphosites, SCAD-Fe-NTA had the highest yield (Fig. 3a, b).

### Identification of New TRPM7 Phosphosites

After comparing phosphosites found in this experiment with previously reported phosphorylated amino acids, we identified six new phosphorylated positions (Fig. 3c and Table S1). All phosphosites were modified serine or threonine residues including positions 5, 233, 554, 824, 1265, and 1401. Of the six newly identified sites, two positions were observed in four out of 12 replicates.

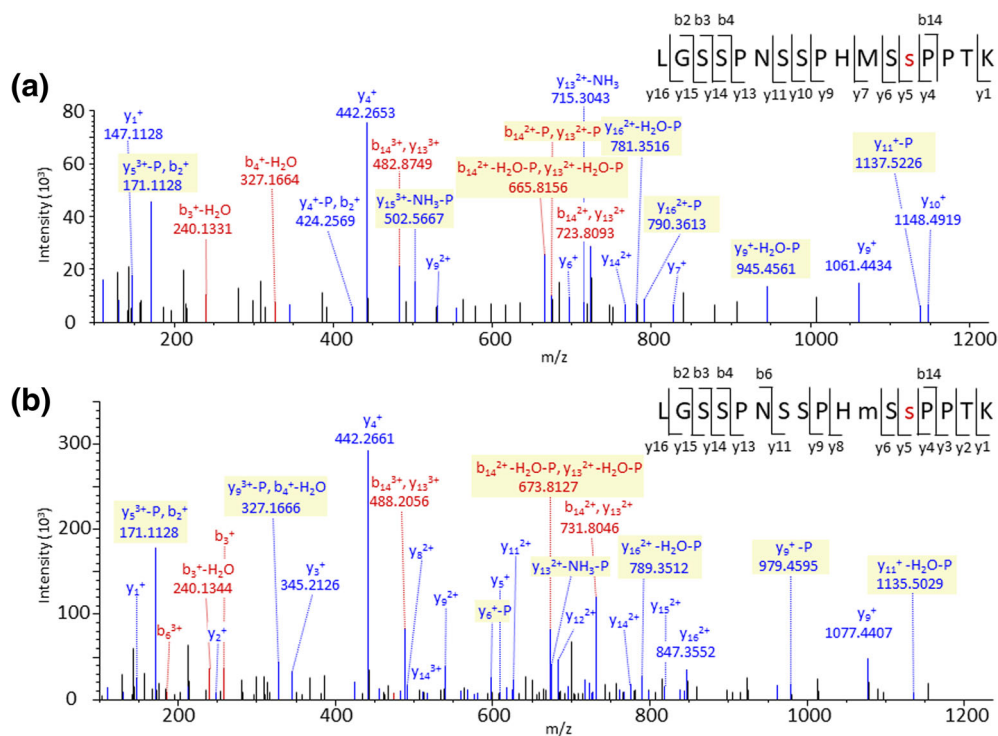
Four standard peptides were evaluated to confirm our results. Two peptides contained clear potential novel positions (S5 and S553). The third was a phosphosite with a low probability ( $X_{corr} < 2$  and  $ptmRS < 95$  or not assigned), namely position S1416. The fourth position compared with a standard was S1395. The whole cell lysate MS/MS spectra were compared with the MS/MS spectra collected for the synthetic peptide standards. Figure 4a contains the annotated MS/MS spectrum for the TRPM7 peptide sWIESTLTK (S5) which is compared with the synthetic standards (Fig. 4b). In addition, the MS/MS spectrum of the synthetic peptide LGSSPNSSPHMSpPTK with S1395 phosphorylated was also collected and compared with the lysate spectrum due to the high number of possible phosphorylated positions on this peptide (Fig. 5a, b). Tandem MS spectra from lysates and synthetic standards for amino acids S5 and S1395 displayed significant overlap (Fig. 4 and Fig. 5). Evaluation of the MS/MS spectra for positions S553 and S1416 was also compared with a



**Figure 4.** Phosphorylated S5 confirmed by synthetic peptide. (a) Tandem mass spectrum of the peptide containing pS5 (SWIESTLTK) compared with (b) a synthetic standard of same sequence

synthetic standard (Fig. S3 and S4); however, S533 phosphorylation was inconclusive and was eliminated from the list of new putative phosphosites. Phosphorylation of S1416 and

S1395 has previously been published [28]. Thus, there is a higher chance of S1416 being phosphorylated than other amino acids on the same peptide, although this cannot be fully



**Figure 5.** Phosphorylated S1395 confirmed by standard peptide. (a) MS/MS spectrum of peptide containing pS1395 (LGSSPNSSPHMSsPPTK) compared with (b) a synthetic standard of same sequence. The standard peptide was also detected with an oxidized methionine at residue 1393, causing a mass shift of 15.99  $m/z$  in some fragments

excluded as a possibility. The annotated MS/MS spectra for the other newly assigned phosphorylation positions including S233, S824, T1265, and S1401 of TRPM7 are included in Figs. S5–9.

### Importance of TRPM7 Phosphorylation

TRPM7 plays a crucial role in cellular processes ranging from individual cellular functions to whole organism development [29–31] with many activities related to its heavy phosphorylation patterns [6, 32–34]. Even though both the S/T rich domain as well as the kinase domain having been analyzed in-depth for phospho-residues [28, 32], TRPM7 is highly phosphorylated and we propose that not all phosphorylation dynamics have been revealed and thus there is still a need for further study. Given this ion channel's wide variety of functions, interacting partners, and substrates, an overall discovery approach to further identify phosphosites at physiological conditions is necessary.

To date, regions between amino acids 1380 to 1548 have been determined to be highly autophosphorylated [32] and are important for the kinase activity of TRPM7. Mutations at S1512 and S1268, as well as S1596 and S1777, lead to a significant decrease in downstream phosphorylation activity by TRPM7 [28, 35]. Substitution of alanine at residue 1616, 1658, 1683, 1693, and 1741 did not result in significant changes in catalytic activities [28]. Additionally, residue S1269 was found to regulate the  $\text{Ca}^{2+}$  influx in a cAMP-dependent manner [36].

In this study, we focused on the isolation of TRPM7 using newly developed extraction and digestion methods as well as detecting phosphorylation amino acids of TRPM7 in physiological conditions. The new phosphosites we found will provide more potential targets for research on functions of this protein.

## Conclusions

Using a combination of SCAD and S-Trap methods proteolytic digestions methods, together with  $\text{TiO}_2$  and Fe-NTA phosphoenrichment methods, we have successfully detected  $22 \pm 6\%$  amino acid sequence coverage of the ion channel TRPM7. With further interest in mapping phosphorylation sites, we were able to identify several modified serine residues, including new sites that had not previously been reported. The analysis of TRPM7 and related modifications provides a means to investigate the functional significance of these phosphorylation sites.

## Acknowledgements

This work was supported by the Department of Chemistry, College of Liberal Arts and Sciences, University of Illinois at Chicago. Financial support was also received from the National Science Foundation (Award# 1655494) and the National Institutes of Health (NIH R56MH107387).

## References

- Wallin, E., von Heijne, G.: Genome-wide analysis of integral membrane proteins from eubacterial, archaean, and eukaryotic organisms. *Protein Sci.* **7**, 1029–1038 (1998)
- Overington, J.P., Al-Lazikani, B., Hopkins, A.L.: How many drug targets are there? *Nat. Rev. Drug Discov.* **5**, 993–996 (2006)
- Kumar, P., Kumar, D., Jha, S.K., Jha, N.K., Ambasta, R.K.: Ion channels in neurological disorders. *Adv. Protein Chem. Struct. Biol.* **103**, 97–136 (2016)
- Lai, T.W., Zhang, S., Wang, Y.T.: Excitotoxicity and stroke: identifying novel targets for neuroprotection. *Prog. Neurobiol.* **115**, 157–188 (2014)
- Aarts, M., Iihara, K., Wei, W.L., Xiong, Z.G., Arundine, M., Cerwinski, W., MacDonald, J.F., Tymianski, M.: A key role for TRPM7 channels in anoxic neuronal death. *Cell.* **115**, 863–877 (2003)
- Visser, D., Middelbeek, J., van Leeuwen, F.N., Jalink, K.: Function and regulation of the channel-kinase TRPM7 in health and disease. *Eur. J. Cell Biol.* **93**, 455–465 (2014)
- Yamaguchi, H., Matsushita, M., Nairn, A.C., Kuriyan, J.: Crystal structure of the atypical protein kinase domain of a TRP channel with phosphotransferase activity. *Mol. Cell.* **7**, 1047–1057 (2001)
- Schmitz, C., Dorovkov, M.V., Zhao, X., Davenport, B.J., Ryazanov, A.G., Perraud, A.L.: The channel kinases TRPM6 and TRPM7 are functionally nonredundant. *J. Biol. Chem.* **280**, 37763–37771 (2005)
- Park, H.S., Hong, C., Kim, B.J., So, I.: The pathophysiological roles of TRPM7 channel. *Korean J. Physiol. Pharmacol.* **18**, 15–23 (2014)
- Hermosura, M.C., Nayakanti, H., Dorovkov, M.V., Calderon, F.R., Ryazanov, A.G., Haymer, D.S., Garruto, R.M.: A TRPM7 variant shows altered sensitivity to magnesium that may contribute to the pathogenesis of two Guamanian neurodegenerative disorders. *Proc. Natl. Acad. Sci. U. S. A.* **102**, 11510–11515 (2005)
- Orwick-Rydmark, M., Arnold, T., Linke, D.: The use of detergents to purify membrane proteins. *Curr. Protoc. Protein Sci.* **84**, 4.8.1–4.8.35. (2016) <https://doi.org/10.1002/0471140864.ps0408s84>
- Tubaon, R.M., Haddad, P.R., Quirino, J.P.: Sample clean-up strategies for ESI mass spectrometry applications in bottom-up proteomics: trends from 2012 to 2016. *Proteomics.* **17**, 1700011 (2017) <https://doi.org/10.1002/pmic.201700011>
- Sun, D., Wang, N., Li, L.: Integrated SDS removal and peptide separation by strong-cation exchange liquid chromatography for SDS-assisted shotgun proteome analysis. *J. Proteome Res.* **11**, 818–828 (2012)
- Zhao, Q., Fang, F., Shan, Y., Sui, Z., Zhao, B., Liang, Z., Zhang, L., Zhang, Y.: In-depth proteome coverage by improving efficiency for membrane proteome analysis. *Anal. Chem.* **89**, 5179–5185 (2017)
- Lee, S.C., Knowles, T.J., Postis, V.L.G., Jamshad, M., Parslow, R.A., Lin, Y.-p., Goldman, A., Sridhar, P., Overduin, M., Muench, S.P., Dafforn, T.R.: A method for detergent-free isolation of membrane proteins in their local lipid environment. *Nat. Protoc.* **11**, 1149 (2016)
- Zougman, A., Selby, P.J., Banks, R.E.: Suspension trapping (S-Trap) sample preparation method for bottom-up proteomics analysis. *Proteomics.* **14**, 1006–1000 (2014)
- Hughes, C.S., Moggridge, S., Muller, T., Sorensen, P.H., Morin, G.B., Krijgsvelde, J.: Single-pot, solid-phase-enhanced sample preparation for proteomics experiments. *Nat. Protoc.* **14**, 68–85 (2019)
- Qualtiere, L.F., Anderson, A.G., Meyers, P.: Effects of ionic and nonionic detergents on antigen-antibody reactions. *J. Immunol.* **119**, 1645–1651 (1977)
- Dimitriadis, G.J.: Effect of detergents on antibody-antigen interaction. *Anal. Biochem.* **98**, 445–451 (1979)
- Ma, F., Liu, F., Xu, W., Li, L.: Surfactant and chaotropic agent assisted sequential extraction/on-pellet digestion (SCAD) for enhanced proteomics. *J. Proteome Res.* **17**, 2744–2754 (2018)
- HaileMariam, M., Eiguez, R.V., Singh, H., Bekele, S., Ameni, G., Pieper, R., Yu, Y.: S-Trap, an ultrafast sample-preparation approach for shotgun proteomics. *J. Proteome Res.* **17**, 2917–2924 (2018)
- Ludwig, K.R., Schroll, M.M., Hummon, A.B.: Comparison of in-solution, FASP, and S-Trap based digestion methods for bottom-up proteomic studies. *J. Proteome Res.* **17**, 2480–2490 (2018)
- Kuroda, H., Kutner, R.H., Bazan, N.G., Reiser, J.: Simplified lentivirus vector production in protein-free media using polyethylenimine-mediated transfection. *J. Virol. Methods.* **157**, 113–121 (2009)



24. Gorman, C.M., Howard, B.H., Reeves, R.: Expression of recombinant plasmids in mammalian cells is enhanced by sodium butyrate. *Nucleic Acids Res.* **11**, 7631–7648 (1983)
25. Parham, J.H., Iannone, M.A., Overton, L.K., Hutchins, J.T.: Optimization of transient gene expression in mammalian cells and potential for scale-up using flow electroporation. *Cytotechnology.* **28**, 147–155 (1998)
26. Kim, T.Y., Shin, S.K., Song, M.Y., Lee, J.E., Park, K.S.: Identification of the phosphorylation sites on intact TRPM7 channels from mammalian cells. *Biochem. Biophys. Res. Commun.* **417**, 1030–1034 (2012)
27. Huttlin, E.L., Jedrychowski, M.P., Elias, J.E., Goswami, T., Rad, R., Beausoleil, S.A., Villen, J., Haas, W., Sowa, M.E., Gygi, S.P.: A tissue-specific atlas of mouse protein phosphorylation and expression. *Cell.* **143**, 1174–1189 (2010)
28. Cai, N., Bai, Z., Nanda, V., Runnels, L.W.: Mass spectrometric analysis of TRPM6 and TRPM7 phosphorylation reveals regulatory mechanisms of the channel-kinases. *Sci. Rep.* **7**, 42739 (2017)
29. Liu, W., Su, L.T., Khadka, D.K., Mezzacappa, C., Komiya, Y., Sato, A., Habas, R., Runnels, L.W.: TRPM7 regulates gastrulation during vertebrate embryogenesis. *Dev. Biol.* **350**, 348–357 (2011)
30. Su, L.T., Liu, W., Chen, H.C., Gonzalez-Pagan, O., Habas, R., Runnels, L.W.: TRPM7 regulates polarized cell movements. *Biochem. J.* **434**, 513–521 (2011)
31. Su, L.T., Agapito, M.A., Li, M., Simonson, W.T., Huttenlocher, A., Habas, R., Yue, L., Runnels, L.W.: TRPM7 regulates cell adhesion by controlling the calcium-dependent protease calpain. *J. Biol. Chem.* **281**, 11260–11270 (2006)
32. Clark, K., Middelbeek, J., Morrice, N.A., Figdor, C.G., Lasonder, E., van Leeuwen, F.N.: Massive autophosphorylation of the Ser/Thr-rich domain controls protein kinase activity of TRPM6 and TRPM7. *PLoS One.* **3**, e1876 (2008)
33. Clark, K., Middelbeek, J., Lasonder, E., Dulyaninova, N.G., Morrice, N.A., Ryazanov, A.G., Bresnick, A.R., Figdor, C.G., van Leeuwen, F.N.: TRPM7 regulates myosin IIA filament stability and protein localization by heavy chain phosphorylation. *J. Mol. Biol.* **378**, 790–803 (2008)
34. Dorovkov, M.V., Ryazanov, A.G.: Phosphorylation of annexin I by TRPM7 channel-kinase. *J. Biol. Chem.* **279**, 50643–50646 (2004)
35. Matsushita, M., Kozak, J.A., Shimizu, Y., McLachlin, D.T., Yamaguchi, H., Wei, F.Y., Tomizawa, K., Matsui, H., Chait, B.T., Cahalan, M.D., Naim, A.C.: Channel function is dissociated from the intrinsic kinase activity and autophosphorylation of TRPM7/ChaK1. *J. Biol. Chem.* **280**, 20793–20803 (2005)
36. Broertjes, J., Klarenbeek, J., Habani, Y., Langeslag, M., Jalink, K.: TRPM7 residue S1269 mediates cAMP dependence of Ca<sup>2+</sup> influx. *PLoS One.* **14**, e0209563 (2019)